

Development of a 3D ground model for an offshore wind farm with complex interlayering of silty soils

Xiuzhong Peng^{1#}, Yaoxiang Gao¹, Yuchen Du², Deyuan Wang², Pengfei Li², Xishuang Li³, and Youhu Zhang¹

¹*School of Civil Engineering, Southeast University, Nanjing 211189, China.*

²*China Nuclear Power Design Co., Ltd. (Shenzhen), Shenzhen 518000, China.*

³*First Institute of Oceanography, Ministry of Natural Resources, Qingdao 266061, China.*

[#]*Corresponding author: pengxiuzhong163@163.com*

ABSTRACT

Three-dimensional (3D) ground models enable the visualization of complex subsurface conditions in offshore wind farms, which aid engineers in understanding the spatial morphologies and interrelations of different soil layers. Due to the large areas of offshore wind farms, 3D ground models established solely based on limited geotechnical data (e.g., boreholes and cone penetration tests) might lack the required accuracy. Geophysical data, particularly seismic profile data, is capable of revealing stratigraphic information and can be obtained at a relatively low cost. This study presents a case study in which a 3D ground model for an offshore wind farm located off the Southern China coast is developed through the integration of geotechnical and geophysical data. The wind farm features complex interlayering of silty materials below the soft Holocene marine deposits due to repeated sea level changes during the Quaternary period. This created significant challenges for developing a reliable ground model. In this paper, the challenges that were faced and solutions that were applied in this project are presented and discussed.

Keywords: offshore wind farm; ground model; geotechnics; geophysics.

1. Introduction

Three-dimensional (3D) ground models achieve the reconstruction of the geomorphology and geological structures through utilizing multiple site investigation data (Rushton and Nguyen 2019). In offshore wind farm (OWF) projects, 3D ground models can provide an overall understanding of geological hazards, seafloor, and stratigraphic features, possessing the potential to save development costs, decrease engineering risks and improve construction efficiency (Klinkvort et al. 2020, Sauvin et al. 2022).

The marine environments are readily susceptible to climatic and hydrodynamic conditions, exhibiting a high degree of complexity (Ge et al. 2022, Lin et al. 2022). In the northern South China Sea, coastal rivers continuously transport abundant detritus to the continental margin, gradually forming extensive fine-grained deposits on the continental shelf (Li, Miao, and Yan 2022). During the Quaternary period, the soil deposits might be heterogeneous in this region due to the interaction of sea-level changes, monsoon currents, and seafloor topography (He et al. 2017). The soil types and sediment distribution demonstrate significant spatial variability, with the complex interlayering of silty soils appearing in local sites. In recent years, China has accelerated the development of green energy and is constructing multiple OWF projects in the northern region of the South China Sea. For these OWFs, the complex marine geological conditions pose challenges to the establishment of 3D ground models.

The integrated interpretation of geotechnical and geophysical data can reduce the uncertainty of marine site investigations and obtain more accurate stratigraphic information (Vanneste et al. 2022, Putri et al. 2023). Geotechnical data, including boreholes and cone penetration tests (CPTs), are limited in quantity but high in precision, generally only reflecting the sub-seafloor conditions at the wind turbine locations (Forsberg et al. 2017). Considering the vast area of an OWF, the geotechnical data alone have difficulties in capturing the stratigraphic variations of the entire field (Reynolds et al. 2017). Geophysical surveys, especially seismic exploration, determine stratigraphic depth through the acoustic reflection at the positions where wave impedance dramatically changes (Vardy 2015). Seismic data, represented as texture images composed of seismic signals, are characterized by wide coverage and low acquisition cost (O'Neill et al. 2023). In the process of the integrated interpretation, the geotechnical data provide the seismic data with the information on soil types and geotechnical properties (Rushton and Nguyen 2019). Meanwhile, seismic data facilitate the extrapolation of geotechnical data to the whole area (Eady, Bloore, and Gerritsma 2023). It was reported that the integrated interpretation technique brought significant economic benefits to the construction of the East Anglia One OWF located in the United Kingdom (Reynolds et al. 2017). During developing the OWF, the total cost of the site investigation was reduced by 10% ~ 15%, and the confidence level of the predicted geotechnical parameters was obviously improved.

However, it is common that the geophysical data are used for modelling by means of human-computer interaction (Turner, Kessler, and van der Meulen 2021). Faced with complex stratigraphic features, the modelling process would heavily rely on the experience of modelers and consume a great deal of time and effort. When new geotechnical and geophysical data becomes available, 3D ground models might be slow in updating and fail to playing the maximum value in the development of OWFs. Therefore, it is necessary to explore novel strategies to improve the modelling efficiency and accuracy under complex geological conditions. There are still multiple challenges in achieving this goal:

- interpretation and accurate description of the site investigation data;
- determination of layer interfaces with efficiency and precision;
- modelling of complex geological bodies.

This study aims at integrating multiple site investigation data to develop a refined 3D ground model for an OWF located in the northern South China Sea. Based on available geological knowledge at this site, an integrated interpretation of geotechnical and geophysical data was conducted to obtain accurate sub-seafloor conditions. Through selecting a reasonable interpolation method, a series of continuous layer interfaces were generated from scattered data points containing stratigraphic information. Subsequently, a modelling technique of complex geological bodies was explored to create a final 3D ground model.

2. Survey area and data

2.1. Site description

The survey area is located on the northern continental shelf of the South China Sea, just east of the Pearl River Estuary, and approximately 22 km from the nearest coast. This area is subject to the East Asian Monsoon with abundant wind energy resources. The monsoon generally blows from the north-east in the winter and from the south-west during the summer. During the Quaternary period, this area was influenced by a combination of sea-level changes and river-discharged sediments, resulting in complex transitional interlayering of silty soils (Li, Miao, and Yan 2022, He et al. 2017).

At the end of 2023, the OWF was completed and started operating. The OWF covers an area of 41 km² and contains 25 wind turbines with a total installed capacity of 300 MW. The location and boundary of the OWF are shown in Fig. 1.

2.2. Geotechnical data

In the geotechnical investigation, geotechnical data were collected near wind turbine locations. Each location had two sampling points, between which the distance was about 20 m ~ 40 m. The investigation included 40 sampling boreholes and 10 CPTs to a target depth of 90 m below the seafloor. The geotechnical data provides information on geological formations from the Late Pleistocene and the Holocene. The location of geotechnical sampling points is presented in Fig. 2.

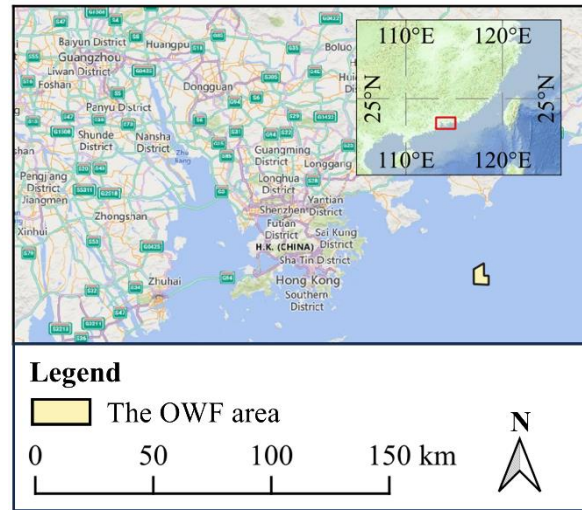


Figure 1. The location and boundary of the Offshore Wind Farm (OWF).

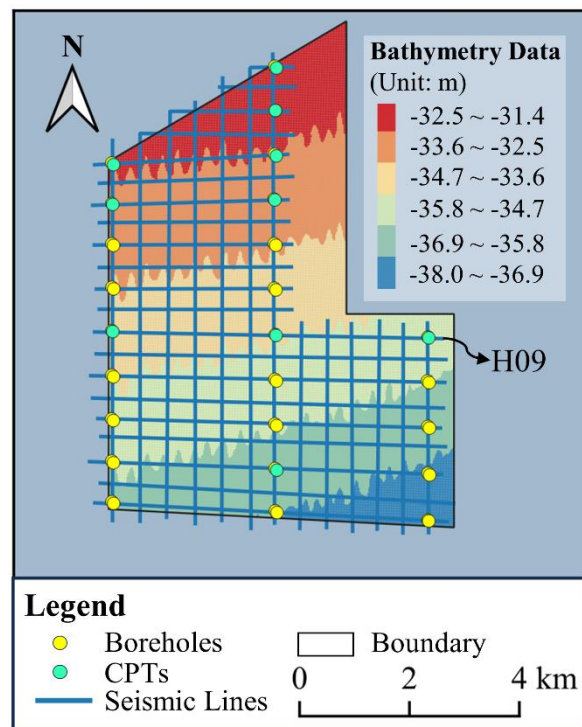


Figure 2. Geotechnical sampling points, 2D seismic lines, and bathymetry data.

2.3. Geophysical data

The marine geophysical surveys, consisting of 2D multi-channel seismic surveys and bathymetry surveys, aimed to acquire stratigraphic depths, sedimentary thicknesses, and seabed geomorphology.

The 2D multi-channel seismic surveys utilized sparker sources and obtained 34 seismic profiles with the penetration of up to 300 ms two-way travel time. In Fig. 2, the 2D seismic lines contain 13 north-south lines (main lines) and 21 east-west lines (cross lines), having a total length of approximately 170 km. The spacing is about 500 m between the main lines and 300 m between the cross lines. Each wind turbine location is traversed by both a main line and a cross line. It is noted that the 2D seismic data covers most of the OWF, except for the northeast corner.

In the bathymetry survey, multibeam echosounder was used to measure the water depth of the OWF. The bathymetry data range from 30 m to 40 m below sea level, as visualized in Fig. 2. It can be observed that the terrain at seabed is flat and gently slopes downward from the north-west to the south-east with an inclination of 0.04 degrees.

3. Ground modelling processes

The modelling processes of 3D ground models are divided into three steps, including data integration, spatial interpolation, and model visualization. Each step attempts to solve a modelling challenge. Data integration aims at leveraging site investigation data to derive sub-seafloor conditions. Spatial interpolation concentrates on accurately predicting the stratigraphic depths at unexplored points and building reliable layer interfaces between adjacent strata. Model visualization intends to achieve the generation of complex geological bodies. The modelling processes of 3D ground models and the corresponding challenges are shown in Fig. 3.

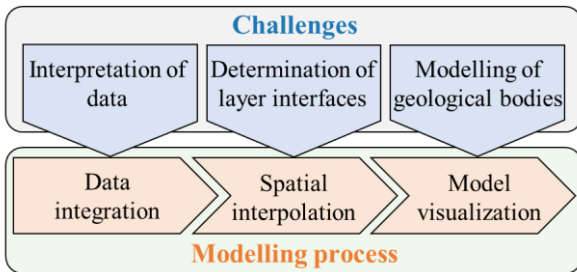


Figure 3. The modelling processes and challenges of 3D ground models.

3.1. Data integration

Data integration means the integrated stratigraphic interpretation of geotechnical and geophysical data, combined with knowledge in local geology to obtain a comprehensive understanding of sub-seafloor conditions (Pearce et al. 2019). Geotechnical data involve the detailed information of soil types and geotechnical properties at sampling locations. Geophysical data provide a solid basis for extrapolating geotechnical data to unexplored locations. For the OWF, this study mainly concentrates on the stratigraphic features within about 90 m below the seafloor. The integration workflow is summarized as follows:

- The locations of geotechnical and seismic data should be accurately marked in a seismic interpretation software. It is necessary to understand the coordinate projection systems used in the data so as to ensure that the data of multiple sources is correctly displayed in the x - y plane. Furthermore, a reasonable acoustic velocity model should be selected to perform time-to-depth conversion for seismic data, establishing the correlation between geotechnical data and seismic data in the z direction. This study utilized an average acoustic velocity of 1600 m/s in sediments to convert the seismic data from the time domain to the depth domain.

- The stratigraphic framework is constructed through the preliminary evaluation of site investigation data. To this end, the comparative analysis of geotechnical data and seismic data is conducted combined with local geological information. The sedimentary interfaces, with significant differences in geotechnical properties and obvious increases in seismic amplitudes, can be identified, providing an analytic framework for integrated interpretation.
- During the integrated interpretation, main strata are initially determined, subsequently followed by identifying localized interlayers. The stratigraphic framework is applied to the interpretation of geotechnical data and seismic data to figure out the main strata and the corresponding geotechnical properties. Within the main strata, clear seismic reflections need to be sought and are compared with geotechnical information to judge whether these reflections are the boundaries of the interlayers. The goal of the integrated interpretation is to achieve the correlation between geotechnical interpretation and seismic stratigraphic interpretation, which is normally a collaborative and iterative process.
- The last step involves examining the consistency of the stratigraphic interpretation results at the intersection of the seismic profiles. If consistency is not achieved, it is essential to find out the reasons and reinterpret the data. When this requirement is met, the data integration is considered complete.

3.2. Spatial interpolation

Spatial interpolation facilitates the generation of a structured grid on a surface from spatially scattered points (Turner, Kessler, and van der Meulen 2021). In general, stratigraphic lines in seismic profiles can be discretized into a series of points with spatial coordinates. These points are spaced closely along seismic lines, leading to the significant accumulation of data. It is necessary to explore spatial interpolation methods appropriate for this specific data distribution to acquire reasonable bounding surfaces.

After examining the various prevalent interpolation techniques to the scattered points derived from stratigraphic lines, it is found that inverse distance weighted (IDW) method (De Mesnard 2013, Ijaz et al. 2023) and kriging method (Shi 2014) exhibit good outcomes. The obtained surfaces are continuous and present acceptable stratigraphic morphologies. Compared with kriging method, IDW method has higher computational efficiency. Consequently, this study adopted the IDW method to generate the grid points on the layer interfaces.

In the IDW method, given N known point coordinates $(x_i, y_i, z_i) (i = 1, 2, \dots, N)$ and an interpolated point location (x, y) , the elevation value z of the interpolated point is expressed as follows (Ijaz et al. 2023):

$$z = \sum_{i=1}^N w_i z_i \quad (1)$$

where w_i denotes the weighting of the i^{th} known point and merely depends on the distance d_i from the interpolated point to the i^{th} known point in the x - y plane. The weighting w_i and the distance d_i are formulated using the following equations (Ijaz et al. 2023):

$$w_i = \frac{(\frac{1}{d_i})^2}{\sum_{i=1}^N (\frac{1}{d_i})^2} \quad (2)$$

$$d_i = \sqrt{(x - x_i)^2 + (y - y_i)^2} \quad (3)$$

In essence, the IDW method is characterized as a linear combination of the elevation values z_i at a group of the known points. Each known point has the corresponding weighting which decreases with the increasing distance d_i . Generally, the IDW method has relatively high accuracy around the known points. However, the interpolation results at a distance from these known points have a tendency to approach the mean elevation values of the surrounding known points, which might deviate from the actual stratigraphic features.

3.3. Model visualization

Model visualization is the process of employing the spatial interpolation results to build a 3D ground model, which achieves the intuitive display of the stratigraphic features below the seafloor. During modelling, the ground model could be separated into multiple individual geological bodies, such as continuous strata and complexly shaped interlayers. Consequently, the key in model visualization is to explore a modelling method for complex geological bodies.

PyVista, an open-source Python library, is suitable for constructing and analysing 3D objects with complex shapes, having the advantages of high modelling efficiency and excellent visual effects (Sullivan and Kaszynski 2019). In this study, PyVista was adopted to create geological bodies and generate a 3D ground model for the OWF. The modelling method of complex geological bodies includes mesh generation and volume cutting, as shown in Fig. 4.

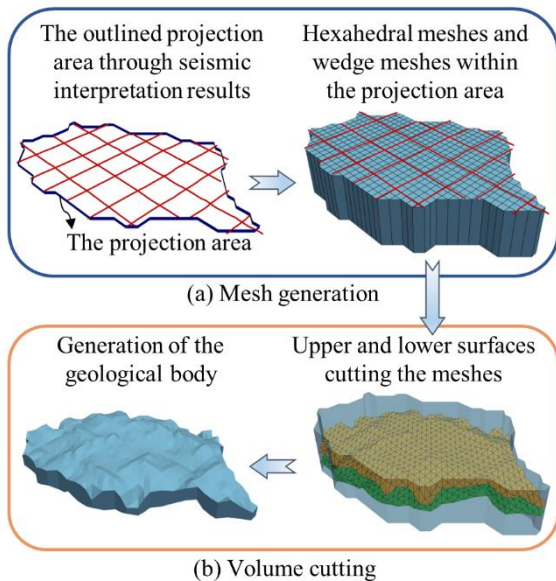


Figure 4. The modelling method of complex geological bodies.

When the seismic lines have proper spacing, the seismic interpretation results could generally outline the projection area of the geological body on the x - y plane. Within this projection area, a group of hexahedral meshes and wedge meshes can be generated using PyVista. The mesh height should be slightly larger than the thickness of the geological body to ensure the geological body can be completely covered. This is depicted in Fig. 4(a). By means of the spatial interpolation technique as discussed in Section 3.2, the upper and lower surfaces of the geological body are obtained. The two surfaces serve the purpose of cutting the meshes to generate the geological body, which is illustrated in Fig. 4(b). This method can realize the 3D modelling of continuous strata and complex interlayers, and the final 3D ground model is formed through assembling of the geological bodies.

4. Results and discussions

4.1. Refined stratigraphy

Taking the seismic line H09 in Fig. 2 as an example, the integrated interpretation results are shown in Fig. 5. Table 1 summaries the geological formations, geotechnical description, and seismic acoustic response for the entire OWF. The seismic line H09, an east-west line, passes through three wind turbine locations, each with a borehole and a CPT. It can be observed from Fig. 5 that there is a strong correlation between the cone resistance and the seismic amplitude, which indicates that it is reasonable to adopt an average acoustic velocity of 1600 m/s in the time-depth conversion. Through the integrated interpretation, the OWF can be divided into five main strata, from shallow to deep, labelled Unit A, Unit B, Unit C, Unit D, and Unit E, respectively. The details on these strata are listed as follows:

- Unit A, Unit B, and Unit C represent muddy clay, silt, and clay, respectively, all of which have low strength. The seismic acoustic responses are all characterized by low amplitude and nearly horizontal internal reflections, showing that these strata have a relatively stable sedimentary environment. In terms of geological conditions, the Unit A and the Unit B belong to the Holocene marine deposits, whereas the Unit C is the Holocene marine-terrestrial transitional phase deposits.
- Unit D features the complex interbedding of silty clay and silty sand. The corresponding geological formation contains the late Pleistocene interactive marine-terrestrial deposits and the Holocene marine-terrestrial transitional deposits. It indicates that the sedimentary conditions within this stratum have changed significantly in geological history, resulting in the highly heterogeneous sediments. In the seismic profile, the horizontal and inclined internal reflections are observed at local positions. Through the combination of the seismic data and geotechnical information, silty clay interlayers and silty sand interlayers could be partially determined from the stratum.

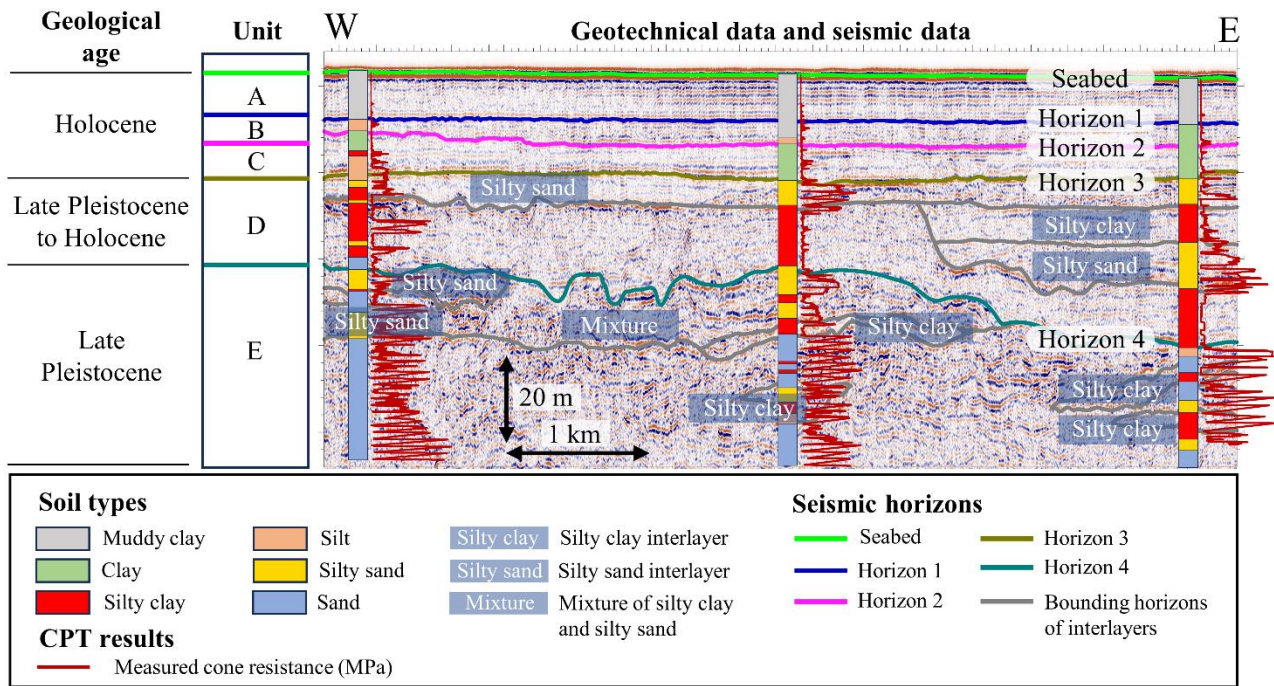


Figure 5. The integrated interpretation results of the seismic line H09.

Table 1. Summary of geological formation, geotechnical description, and seismic acoustic response at the OWF.

Unit	Geological Formation	Geotechnical Description	Seismic Acoustic Response
A	Marine deposits (Holocene)	Very soft muddy clay with extremely low strength	Low amplitude; locally clear horizontal internal reflections
B	Marine deposits (Holocene)	Very soft silt with low strength	Low amplitude; approximately horizontal internal reflectors
C	Marine-terrestrial transitional deposits (Holocene)	Very soft to soft clay with low to medium strength	Low amplitude; approximately horizontal internal reflectors
D	Interactive marine-terrestrial deposits to marine-terrestrial transitional deposits (Late Pleistocene to Holocene)	Interbedding of soft, medium strength silty clay and medium dense to dense silty sand	Moderate amplitude; Structureless with locally horizontal and inclined internal reflectors
E	Interactive marine-terrestrial deposits (Late Pleistocene)	Dense sand with laminae and lenses of firm to stiff, medium to high strength silty clay	Structureless with numerous high amplitude internal reflectors

- Unit E, mainly composed of sand and silty clay, belongs to the late Pleistocene interactive marine-terrestrial deposits. From the seismic acoustic response, numerous high-amplitude reflections can be found within the stratum, exhibiting the complex structural features. In the integrated interpretation results, the Unit E is further subdivided into the upper layer and the lower layer. The upper layer involves a mixture of silty sand and silty clay with silty sand interlayers as well as silty clay interlayers. The lower layer is primarily sand with discrete silty clay lenses.

As shown in Fig. 5, the seismic horizons sometimes have difficulties in coinciding with the geotechnical interfaces. This is because there is a 10 m to 20 m offset between the seismic lines and the actual geotechnical sampling points. Meanwhile, an average acoustic velocity was used in the time-depth conversion.

4.2. Layer interfaces

In Fig. 5, the primary seismic horizons below the seafloor, from shallow to deep, are represented by Horizon 1, Horizon 2, Horizon 3, and Horizon 4. Combined with these seismic horizons in different seismic lines, the IDW method was employed to calculate the elevation at interpolation points of the main layer interfaces. The interpolation results are visualized in Fig. 6. The Horizon 1 and the Horizon 2 exhibit a gradual rise in the terrain from the south-east to the north-west, having a similar structure to the seafloor. In the northern Horizon 3, a narrow depression with an east-west orientation can be observed, whereas an extensive depression oriented from the north-east to the south-west is noticeable in the southern Horizon 4. These depressions could potentially represent ancient riverbeds.

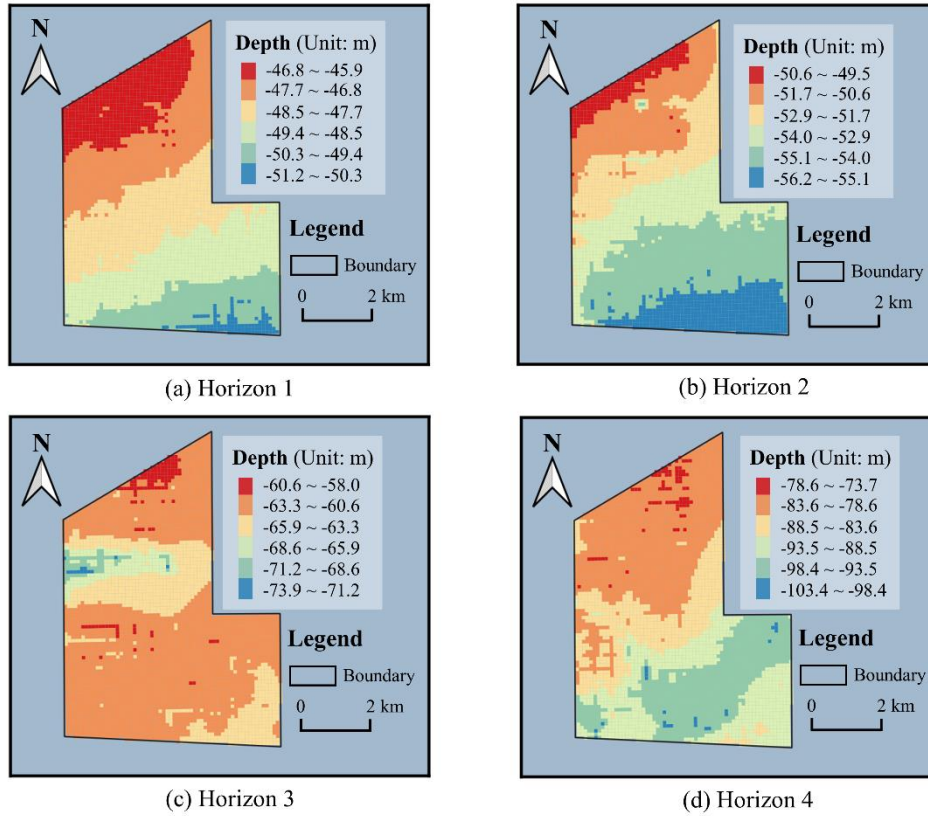


Figure 6. The interpolation results of the main layer interfaces using the inverse distance weighted (IDW) method (Interpolation bin size: $100\text{ m} \times 100\text{ m}$).

Fig. 7 constructs a 3D model of an interlayer through the IDW method. However, the resultant model shows two anomalies in appearance:

- the surfaces of the interlayer have local extrema at the locations of seismic lines, which is presented as local stripes in Fig. 6;
- the edges of the interlayer exhibit distinct fluctuations without the expected pinch-out phenomenon.

These might be attributed to the fact that the IDW method has limitations on capturing the holistic shape features implied by the raw data. Consequently, it would be valuable to improve the IDW method or explore new interpolation strategies to obtain more realistic surfaces of stratum and interlayers.

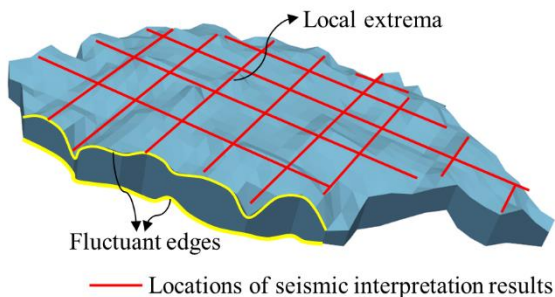


Figure 7. The 3D model of an interlayer through the IDW method (Interpolation bin size: $100\text{ m} \times 100\text{ m}$).

4.3. 3D ground model

The final 3D geological model of the OWF is shown in Fig. 8. Fig. 8(a) depicts the 3D ground model consisting of five main strata. Fig. 8(b) indicates that the Unit A and the Unit B have relatively uniform thickness within the range of the OWF. There exists a slightly thicker clay sediment in the northern Unit C due to the depression of the lower stratum. Fig. 8(c) illustrates the stratigraphic structure within the Unit D. At the top of the stratum, silty clay interlayers and silty sand interlayers are present, forming a layered stacking in the northeastern area of the stratum. In addition, a silty sand interlayer has been identified at the bottom of this stratum. Fig. 8(d) shows the complex internal features of Unit E. The upper layer exhibits the mixed sediment of silty clay and silty sand, with silty clay interlayers and silty sand interlayers discerned at local positions. The lower layer is primarily composed of sand, interspersed with silty clay lenses. As a result, the established 3D ground model has clear visual effects and intuitively displays the overall stratigraphic features.

Nevertheless, it can be seen from Fig. 4 that the projected boundaries of the geological body on the x - y plane remain relatively rough, having a few discrepancies with the anticipated contour outlined by the seismic interpretation results. It is necessary to refine the modelling method of complex geological bodies to reveal more details of the stratigraphic morphology.

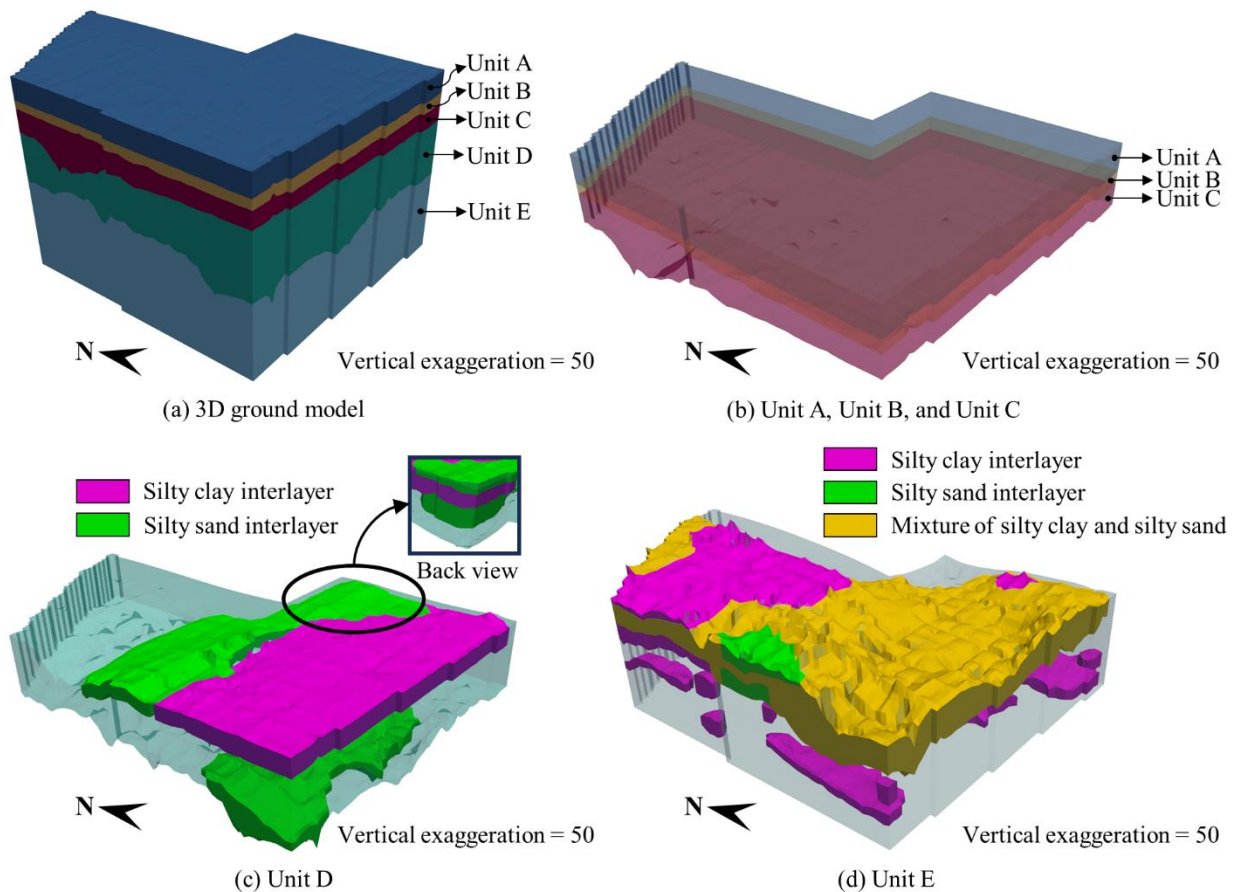


Figure 8. The final 3D ground model for the OWF.

5. Concluding remarks and future work

This study presents an example of leveraging geotechnical and physical data to build a three-dimensional (3D) ground model for an offshore wind farm (OWF) with complex interlayering of silty soils. The modelling process includes data integration, spatial interpolation, and model visualization. This integrated interpretation of the site investigation data focused on the Quaternary sediments within a range of nearly 90 m below the seafloor, and ultimately identified five main strata as well as multiple interlayers. Afterwards, the inverse distance weighting (IDW) method was employed to construct continuous layer interfaces. On this basis, an available Python library named PyVista was utilized to explore a modelling technique of complex geological bodies, achieving the visualization of 3D ground models. Although the resulting ground model has acceptable visual effects, there is still room for improvement in the modelling efficiency and precision.

Future work would concentrate on the refinement of these modelling methods, which are summarized below:

- Seismic inversion is scheduled for application on seismic profiles to derive wave impedance and Q factors, which is expected to validate and adjust the previous data interpretation.
- The IDW method has difficulties in capturing the realistic stratigraphic morphologies. A novel interpolation method should be developed to match the site investigation data that are closely spaced along seismic lines and generate

stratigraphic layer interfaces reflecting holistic geological features.

- The present technique to create complex geological bodies requires to be enhanced to describe more details on stratigraphic morphologies.

Acknowledgements

The authors are grateful for the financial support and data contributions provided by China Nuclear Power Design Co., Ltd. (Shenzhen).

References

- De Mesnard, L. 2013. "Pollution Models and Inverse Distance Weighting: Some Critical Remarks." *Comput Geosci*, 52, 459-469, <https://doi.org/10.1016/j.cageo.2012.11.002>
- Eady, H., C. Bloore, and D. Gerritsma. 2023. "IJmuiden Ver Windfarm Zone: Increasing the Resolution of the Southern North Sea Stratigraphy Using Iterative Ground Modelling Techniques." In: *The 9th International Offshore Site Investigation and Geotechnics Conference*, London, UK, 2072–2079.
- Forsberg, C. F., T. Lunne, M. Vanneste, L. James, T. I. Tjelta, A. Barwise, and C. Duffy. 2017. "Stochastic CPTS from Intelligent Ground Models Based on the Integration of Geology, Geotectonics and Geophysics as a Tool for Conceptual Foundation Design and Soil Investigation Planning." In: *The 8th International Offshore Site Investigation and Geotechnics Conference*, London, UK, 1254-1259, <https://doi.org/10.3723/OSIG17.1254>
- Ge, J., X. Zhao, M. Tan, H. Zhuo, C. Liu, and B. G. Jones. 2022. "Sequence Stratigraphy and Depositional Evolution of

- the North-Eastern Shelf (33.9–10.5 Ma) of the Pearl River Mouth Basin, South China Sea.” *Mar Pet Geol*, 141, 105697, <https://doi.org/10.1016/j.marpetgeo.2022.105697>
- He, M., H. Zhuo, W. Chen, Y. Wang, J. Du, L. Liu, L. Wang, and H. Wan. 2017. “Sequence Stratigraphy and Depositional Architecture of the Pearl River Delta System, Northern South China Sea: an Interactive Response to Sea Level, Tectonics and Paleoclimatology.” *Mar Pet Geol*, 84, 76-101, <https://doi.org/10.1016/j.marpetgeo.2017.03.022>
- Ijaz, Z., C. Zhao, N. Ijaz, Z. U. Rehman, A. Ijaz, and M. F. Junaid. 2023. “Geospatial Modeling of Heterogeneous Geotechnical Data Using Conventional and Enhanced Conception of Modified Shepard Method-Based IDW Algorithms: Application and Appraisal.” *Bull Eng Geol Environ*, 82, 428, <https://doi.org/10.1007/s10064-023-03435-6>
- Li, G., L. Miao, and W. Yan. 2022. “Holocene Evolution of the Shelf Mud Deposits in the North-Western South China Sea.” *Front Mar Sci*, 9, 937616, <https://doi.org/10.3389/fmars.2022.937616>
- Lin, P., X. Xu, C. Yan, L. Luo, M. Abbas, and Z. Lai. 2022. “Holocene Sedimentary of the Pearl River Delta in South China: OSL and Radiocarbon Dating of Cores from Zhuhai.” *Front Mar Sci*, 9, 1031456, <https://doi.org/10.3389/fmars.2022.1031456>
- Klinkvort, R. T., G. Sauvin, C. F. Forsberg, and M. Vanneste. 2020. “Integrated Ground Modelling from a Geotechnical Perspective.” In: *The 4th International Symposium on Frontiers in Offshore Geotechnics*, Austin, Texas, USA, 917-926.
- O'Neill, M. P., A. L. Osuchowski, Y. Cai, M. F. Bransby, P. G. Watson, C. Gaudin, J. Doherty, E. Dalgaard, and R. Ross. 2023. “Integrated and Data Science-Informed Seabed Characterisation for Optimised Foundation Design.” *Ocean Eng*, 284, 115095, <https://doi.org/10.1016/j.oceaneng.2023.115095>
- Pearce, S. D., C. Kilsby, F. J. King, and L. Jones. 2019. “Efficient Design and Execution of Site Investigations for Offshore Wind Farms: Learning from Experience.” In: *Offshore Technology Conference*, Houston, Texas, USA, OTC-29276-MS, <https://doi.org/10.4043/29276-MS>
- Putri, S.A., M. Panggeleng, M. Nauw, A. Maulana, and L. Bachtiar. 2023. “Unlocking the Shallow Overburden Understanding of Ubadari Gas Field in Indonesia Using High-Resolution Shallow Datasets.” In: *The 9th International Offshore Site Investigation and Geotechnics Conference*, London, UK, 2129–2136.
- Reynolds, J. M., L. M. L. Catt, A. B. Fernandes, and P. Knight. 2017. “Development of 3D Ground Models for Offshore Wind Farms – Rhiannon OWF, Irish Sea.” In: *The 9th International Offshore Site Investigation and Geotechnics Conference*, London, UK, 1307-1314, <https://doi.org/10.3723/OSIG17.1307>
- Reynolds, J. M., L. M. L. Catt, G. Salaün, P. Knight, W. Cleverly, and L. Costa. 2017. “Integration of Geophysical, Geological and Geotechnical Data for Offshore Wind Farms – East Anglia One OWF, Southern North Sea, A Case History.” In: *The 9th International Offshore Site Investigation and Geotechnics Conference*, London, UK, 1291-1298, <https://doi.org/10.3723/OSIG17.1291>
- Rushton, D. and M. Nguyen. 2019. “On the Application and Benefits of an Integrated Geophysical and Geotechnical Digital Ground Model to Optimize a Site Investigation Survey for an Offshore Wind Farm Project.” In: *The 4th International Conference on Geotechnics for Sustainable Infrastructure Development*, Hanoi, Vietnam, 1337-1344, https://doi.org/10.1007/978-981-15-2184-3_175
- Sauvin, G., M. Vardy, R. T. Klinkvort, M. Vanneste, C. F. Forsberg, and A. Kort. 2022. “State-of-the-Art Ground Model Development for Offshore Renewables – TNW Case Study.” In: *EAGE GET 2022*, Hague, Netherlands, 1-5, <https://doi.org/10.3997/2214-4609.202221109>
- Shi, G. 2014. “Chapter 8 - Kriging.” In: *Data Mining and Knowledge Discovery for Geoscientists*, Elsevier, Amsterdam, Netherlands, 238-274, <https://doi.org/10.1016/B978-0-12-410437-2.00008-4>
- Sullivan, C. and A. A. Kaszynski. 2019. “PyVista: 3D Plotting and Mesh Analysis through a Streamlined Interface for the Visualization Toolkit (VTK).” *J Open Source Softw*, 4(37), 1450, <https://doi.org/10.21105/joss.01450>
- Turner, A. K., H. Kessler, and M. J. van der Meulen. 2021. “Applied Multidimensional Geological Modeling: Informing Sustainable Human Interactions with the Shallow Subsurface.” John Wiley & Sons Ltd, West Sus, UK, <https://doi.org/10.1002/9781119163091>
- Vanneste, M., G. Sauvin, J.-R. Dujardin, C. F. Forsberg, R. T. Klinkvort, C. S. Forsberg, and R. C. Hansen. 2022. “Data-Driven Ground Models: The Road to Fully-Integrated Site Characterization and Design.” In: *The 2nd Vietnam Symposium on Advances in Offshore Engineering*, Ho Chi Minh City, Vietnam, 3-21, https://doi.org/10.1007/978-981-16-7735-9_1
- Vardy, M. E. 2015. “Deriving Shallow-Water Sediment Properties Using Post-Stack Acoustic Impedance Inversion.” *Near Surf Geophys*, 13(2), 143-154, <https://doi.org/10.3997/1873-0604.2014045>